Iranian Journal of Electrical and Electronic Engineering 01 (2020) 122–129
Special Issue on Electrical Machines and Drives

IUST
Iran University of Science and Technology

Iranian Journal of Electrical and Electronic Engineering

Journal Homepage: ijeee.iust.ac.ir

Research Paper

Torque Ripple Reduction in Switched Reluctance Motors by Rotor Poles Shape and Excitation Pulse Width Modification

H. Davari* and Y. Alinejad-Beromi*(C.A.)

Abstract: In this paper, at first, a 24/16 three-phase switched reluctance motor is designed, then the rotor poles shape tips corrected for reduction ripple of single-phase torque waveform. By doing this, the single-phase torque waveform has a flat surface and consequently, the single-phase torque ripple is reduced. Also, due to the commutation between the machine phases, the torque drops during this time, which are known as torque pits. To reduce the ripple torque at these points, which requires overlap between the two successive phases of the machine, the pulse width of the excitation of the machine phases is adjusted. Comparisons have been made between two types of direct current excitation and chopped current (with different pulse widths). The results show that for constant pulse width under chopped current, applying the arc and modifying the shape of the rotor poles can reduce the torque ripple by 3.4%. Also, by applying chopped current control, the torque ripple was reduced by 46.7% compared to its conventional design structure.

Keywords: Non-Uniform Air Gap, Pole Shape, Switched Reluctance Motor, Torque Ripple.

1 Introduction

SWITCHED reluctance motors are a type of modern electric motors, which in recent years had been precisely controlled and drive by advances in power electronics. These motors are simple and robust in structure and due to the lack of winding and a permanent magnet in their rotor compartment, they can be used in high-temperature locations as well as at high speeds. The absence of a permanent magnet or winding in the rotor section causes the torque of these motors to be reluctance torque by varying the air gap between the stator and the rotor. Also, the core structure of the switched reluctance motors is salient at both sides of the stator and rotor, in which the winding is concentrated type only in the stator side. One of the major drawbacks of these motors is having a significant ripple in the output torque. Various methods have been proposed to reduce the torque ripple of these motors, in [1] by creating barriers flux in the rotor, the torque ripple slightly reduced, in [2] by optimizing the stator and rotor pole arcs, the torque ripple is reduced.

In [3] a rotor's structure with a slotted pole or pointed spindle pole in the direction of motor rotation has been proposed that decreases the torque ripple of the machine by about 4.4% by reducing the dispersion flux. Also in [4], the same method is presented on a mutually copulated motor. In [5], with the change in the shape of the stator and rotor teeth, the single-phase torque waveform of the machine is modified and eventually, the ripple torque is reduced. In addition to these references, in [6] a form of stator' poles with non-uniform air gap with a pole shoe attached to the rotor's pole is presented to reduce the torque ripple, the torque has been reduced by 23% compared to the conventional design. In References [7, 8] by modifying the rotor pole step and stepping on the rotor pole forehead, which are both used for low-pole motors and high-speed motors, have reduced the torque ripple, respectively. In [9], in order to decrease the torque ripple, a multilayer motor structure is proposed. Some other studies, such as [10], have used a rotor with more poles than stator to reduce the torque ripple. In [11], the effect of changing in the displacement of the bonding hole for core laminations

Iranian Journal of Electrical and Electronic Engineering, 2020.
Paper first received 06 October 2019, revised 11 November 2019, and accepted 16 November 2019.
* The authors are with the Electrical & Computer Engineering Faculty, Semnan University, Semnan, Iran.
E-mails: h.davari@semnan.ac.ir and yalinejad@semnan.ac.ir.
Corresponding Author: Y. Alinejad-Beromi.

on Ripple torque reduction is investigated. References [12, 13] have proposed a mechanical offset in two-stator machines to reduce the torque ripple for radial and axial flux structures, respectively. Reference [14] has investigated the reduction of torque ripple by applying parametric sweep and optimization on some design parameters of a 24/16 tooth structure. As has been known from previous researches, various methods have been employed to reduce torque ripple of SRMs, but the issue of torque ripple reduction is still one of the most important research areas for switched reluctance motors, as the problem of torque ripple is still present.

In this paper, at first, a switched reluctance motor with 24/16 poles arrangement is designed and optimized with the design of experimental (DoE) by finite element software, then by changing in the forehead surface of the rotor pole, it has been tried to reduce torque ripple. Finally, the best pulse width was selected to excite each phase of the machine to reduce the torque ripple caused by the commutation point. In Sections 2 and 3, the torque ripple reduction method and description of the design are given, respectively. Section 4 provides results and comparisons, and finally, Section 5 conclusion is presented.

2 Torque Ripple Reduction Method

The torque ripple of the switched reluctance motors is divided into two parts, the first part is related to single-phase torque waveform and the second part is related to the commutation region. The first part is modified by changing the shape of the rotor poles and the second part is modified by changing the pulse width of the excitation of each phase of the machine. The general relationship of the output torque of the three-phase switched reluctance machine is as (1).

$$T = \frac{1}{2} i_a^2 \frac{\partial L_a}{\partial \theta} + \frac{1}{2} i_b^2 \frac{\partial L_b}{\partial \theta} + \frac{1}{2} i_c^2 \frac{\partial L_c}{\partial \theta} \quad (1)$$

In this equation, L_a, L_b, and L_c are self-inductances of the three-phase machine, respectively, as well as i_a , i_b and i_c are three-phase currents of the machine.

2.1 Single-phase torque ripple reduction

As the current is attempted to remain constant during the conduction of each phase of the machine, so this torque is directly followed by the derivative of the self-inductance curve of each phase (according to (1)). As the air gap between the stator and rotor poles continuously decreases from the start of the overlap to the complete overlap between the rotor and stator poles, the total flux density of the machine increases with increasing overlap. During this time the density of the tangential flux decreases and the radial flux density increases [15]. The single-phase torque equation (2) is expressed in terms of air-gap distance δ, axial length of the core L, rotational radius or outer radius of the rotor r, air magnetic permeability coefficient μ_0, and density of the air gap flux B_g [16].

$$T = \frac{\delta L r}{2\mu_0} B_{g(\delta,\theta,i)}^2 \quad (2)$$

As it is known, with increasing overlap between poles and decreasing the air gap length, the amount of single-phase torque decreases due to the decreasing in the tangential flux density of the air gap. So during this time, the output torque, which is equal to the torque of one phase of the machine, first ascends, then has to remain constant for a while, eventually declining to zero, but in practice it has been observed that the torque does not remain constant due to the continuous decreasing in air gap length and tangential flux density changes and it decreases with a slight slope, so that cause torque ripple.

The idea of this paper is to reduce the total torque ripple which is related to the single-phase torque. This can be done by elimination the partial part of the rotor pole in the rotational direction and creation of a non-uniform air gap under the full aligned condition of the poles. This action causes a gradual reduction of the air gap length and it also makes the inductance waveform more linear. The linearization of the inductance waveform means that the slope of the curve remains constant during positive motor operation, while in normal conditions, the inductance waveform slightly curved in the areas around aligned and unaligned of the stator and rotor poles. Since the motor torque is directly proportional to the inductance derivative and because it tries to keep the current constant during single-phase conduction, therefore reducing the inductance derivative changes causes decreasing of single-phase torque ripple.

2.2 Torque Ripple Reduction in Commutation Region

In the commutation zone, due to turning off of the excitation for one of the phases, the phase current decreases. Simultaneously, with excitation of the next phase, the phase current also ascends, but due to the inductive-resistive property of the machine winding, the declining and the ascending currents occur with delay. This has a direct impact on the torque waveform of both consecutive phases of the machine. So the resulting torque according to (1) has dips in the zones between the two successive phases, known as torque pits.

These pits create torque ripple in the commutation zones of the machine phases. A slight overlap between the two-phase excitation of the machine helps to reduce the drop in this part of the machine's torque. By changing the pulse width corresponding to the excitation of each phase of the machine, the overlap between the two successive phases can be changed. By choosing the best pulse width, the torque ripple due to commutation is reduced. With the best values selections

of both parts, the total torque ripple can be greatly reduced.

3 Switched Reluctance Motor Design

At first, a conventional structure of a 24/16 switched reluctance three-phase motor arrangement was selected using the explanations presented in [16-19]. This design has been optimized with the Design of Experimental (DoE) method using finite element software. Fig. 1 illustrates the structure and the parameters of the motor considered in this research. In this figure, β_s and β_r are the stator and rotor poles, D_s and $D_{s_{in}}$ are the outer diameter and the inner diameter of the stator core, D_r and $D_{r_{in}}$ are the outer diameter and the inner diameter of the rotor core, h_s and h_r are the heights of the stator and rotor poles, t_s and t_r are the widths of the stator and rotor poles, y_s and y_r are the yoke widths of the stator and rotor, respectively. Also, δ is the length of the air gap between the stator and the rotor in complete aligned condition. The winding of the machine is concentrated type as shown in Fig. 2, so that each tooth forms a pole.

In the design method, the values of parameters such as the stator and rotor pole arcs are provided by Lawrenson's feasible triangle [20], also the main dimensions of the motor such as axial length and crater diameter determined from the torque per unit rotor volume table and shear stress presented in [21] (output torque equation of the machine that relates the dimensions of the machine to the output torque is used). The rest of the design issues have been applied as described in the references.

The optimization performed by the design of the experimental (DoE) method was carried out with the aim of achieving higher than 80% efficiency, average torque of 2Nm and a rated speed of 1500rpm. The weight of all these optimization goals is considered equal to one. Table 1 shows the design parameters of the machine. the material used in the core of this motor is M19-29G steel type, with a saturation of about 1.8 Tesla.

The selected 24/16 SRM is one of the most suitable motor designs for having the lowest output torque ripple as far as its structure is concerned. In fact, this structure has a small stroke angle due to the large number of stator and rotor poles, which has the lowest value compared to other three-phase arrangements. Therefore, in this paper, this structure is used to apply some deformation to the rotor teeth. Fig. 3 shows the deformation performed on the rotor poles to reduce single-phase torque ripples. The angle α is defined as the angle of the arc deviation of the rotor pole forehead.

By increasing this angle, the deviation of this arc increases and eventually causes a more non-uniform air gap in the aligned position. By performing a parametric sweep of α, different waveforms of single-phase torque can be generated. Finally, by comparing the ripple value of these waveforms, the angle corresponding to the minimum single-phase torque ripple is chosen as the angle applied to the rotor poles. This change in rotor pole face causes to smooth self-inductance derivative waveform of the motor, thereby this work eliminates the slope of the torque waveform caused by a phase of the motor. In this method, a number of points (x_1 up to x_n) are selected based on the angle α on the circular curve to the center of the point A, then an arc is drawn from the center of each of these points with the radius of that points until point A. As the angle α becomes larger, the curvature of the arc of the rotor pole is further increased. By simulating all of these schemes individually, some data corresponding to the slope of the single-phase torque waveform are obtained, by comparing them, a point with the least single-phase torque ripple is selected.

4 Simulation Results

By performing finite element simulations, a total of 20 states with 0.1 degree steps (from 0 to 2 degrees) are considered. In order to compare these arcs, a single-phase torque diagram in the presence of a constant current of 1A was used.

Results of the single-phase waveform with the effect of the angle change on the rotor pole forehead by applying 1A to the windings of the machine are shown in Fig. 4. The average and peak-to-peak variations of the single-phase torque waveform and the single-phase torque

Table 1 Design parameters of the machine.

Number of stator pole	24
Number of rotor pole	16
Air gap length	0.46 mm
Axial length of core	86 mm
Outer diameter of stator	145 mm
Inner diameter of stator	84.92 mm
Stator pole arc	7.8°
Rotor pole arc	10.125°
Stator yoke width	5 mm
Rotor yoke width	5 mm
Operational voltage	220 V
Output power	348.41 W
Rotor speed	1500 rpm
Number of turn per pole	54

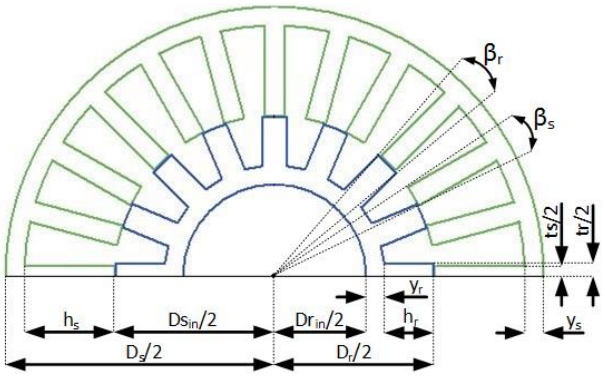

Fig. 1 Design parameters.

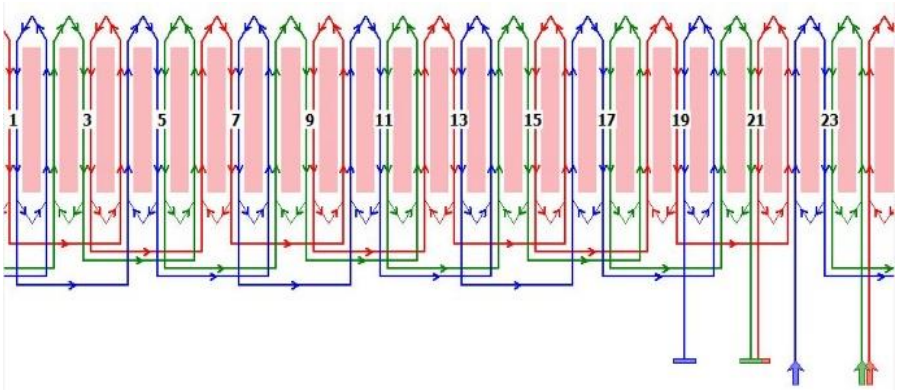

Fig. 2 Stator windings of the machine.

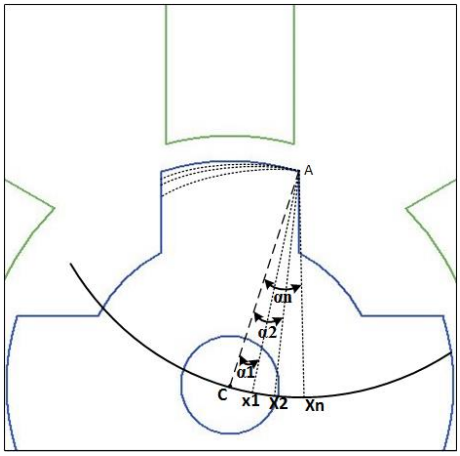

Fig. 3 Rotor pole deformation.

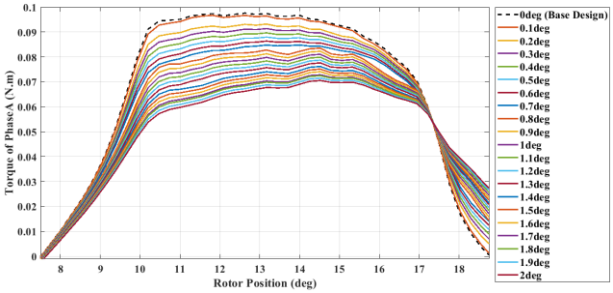

Fig. 4 Single-phase torque waveform for different α angle.

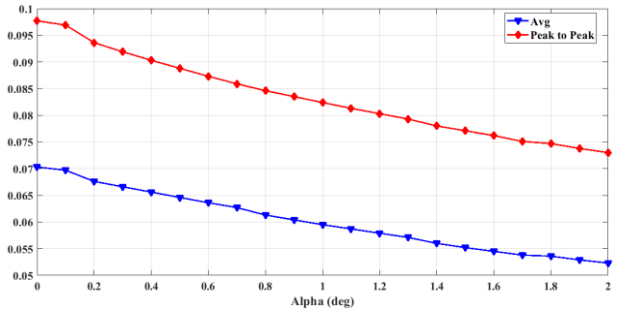

Fig. 5 Average and peak-to-peak variations of single-phase torque waveforms in terms of α angle.

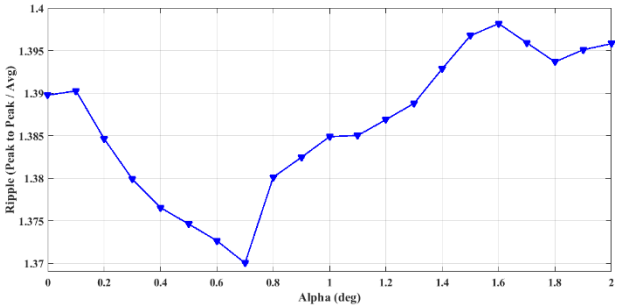

Fig. 6 Single-phase torque ripple variations in terms of α angle.

ripple values are shown in Figs. 5 and 6, respectively. It is shown in Fig. 6 that for an angle equal to 0.7 degrees, the amount of single-phase torque ripple is minimized. The single-phase torque ripple value is calculated from (3) by having average and peak-to-peak values of single-phase waveforms.

All simulations were performed by ANSYS Maxwell software, also Motor-cad software was used to draw the stator winding arrangement.

$$\text{Ripple}=\frac{\text{Max-Min}}{\text{Avg}}=\frac{\text{Peak to Peak}}{\text{Avg}} \tag{3}$$

Fig. 7 shows a comparison of the waveform of inductance, inductance derivative and single-phase torque at angles of zero (blue line) and 0.7° (red line).

By comparing these figures, it can be seen that the average amount of torque decreased about 10.8% by applying this angle. It is also observed that the torque waveform by applying this angle in the single-phase conduction region produces a constant single-phase torque, while in conventional motor with 0° angle, the torque waveform has some slope.

In order to keep the phase current constant during the conduction of that phase, the current chopping control technique has been used. Also, to reduce the torque ripple caused by the commutation region, the phase excitation pulse width is selected as the variable parameter in order to achieve the lowest torque ripple. The stroke angle of the 24/16 structure according to reference [22] is equal to 7.5 degrees, the maximum angle for this structure is 11.25 degrees. Therefore, the applied pulse width must vary between these two values. Fig. 8 shows torque waveforms of the machine

Table 2 Average, peak to peak and ripple in terms of different pulse width.

Pulse width [deg]	Average torque [N.m]	Peak to peak torque [N.m]	Ripple
7.5	1.9119	1.2449	0.6511
8	1.9650	1.1215	0.5707
8.5	2.0272	0.8315	0.4101
9	2.0633	0.4793	0.2322
9.5	2.0825	0.5719	0.2746
10	2.0670	0.7534	0.3644
10.5	1.9977	0.9112	0.4561
11	1.8404	1.1333	0.6157

Table 3 Comparison between average, peak to peak and ripple of torque for variation of α angle and pulse width with DC and CCC mode.

	Average torque [N.m]	Peak to peak of torque [N.m]	Ripple [%]
$\alpha = 0$ DC mode	2.21	1.51	69.9
$\alpha = 0.7$ DC mode	2.31	1.61	68.9
$\alpha = 0.7$ CCC mode PW = 7.5°	1.91	1.24	65.1
$\alpha = 0.7$ CCC mode PW = 9°	2.06	0.47	23.2

Table 4 Effect of arc (α angle) variation on average, peak to peak and ripple of torque.

	Average torque [N.m]	Peak to peak of torque [N.m]	Ripple [%]
$\alpha = 0$ CCC mode PW = 9°	2.2172	0.5907	26.64
$\alpha = 0.7$ CCC mode PW = 9°	2.0633	0.4793	23.22

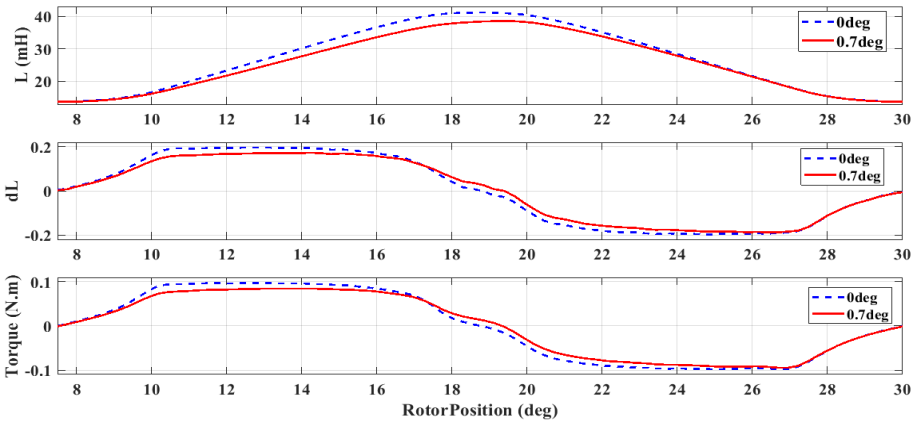

Fig. 7 Comparison of inductance, inductance derivatives and single-phase torque waveforms in design with α angle of zero and 0.7 degrees.

under pulse width changes, also Table 2 shows the average, peak to peak and torque ripple results in terms of pulse width changes.

As shown in Table 2, it is found that for a pulse width of 9 degrees, the torque ripple is minimized, so this value is used. Table 3 also shows the effect of the arc (α angle) applied to the rotor pole under direct current stimulation and the effect of different pulse widths under current chopping control (CCC).

Comparison of the torque ripple between conventional design ($\alpha = 0$) under direct current (DC) and the design with the modified rotor structure ($\alpha = 0.7$) shows that the torque ripple is reduced by one percent. Also, the comparison of torque ripple between conventional design ($\alpha = 0$) under direct current and design with modified rotor structure ($\alpha = 0.7$) under chopping current with 9 degrees pulse width shows that torque ripple decreased by 46.7%.

Table 4 shows the effect of the arc (α angle) applied to the rotor pole under current chopping control. According to the obtained values, it is evident that applying the arc (α angle) on the rotor pole in direction of rotation and under current chopping excitation, the torque ripple reduced by 3.4% which was more effective than direct current excitation to reduce the torque ripple. Fig. 9 shows torque waveforms for pulse widths show in Table 4.

5 Conclusion

In this paper, a 24/16 pole SRM with some modification in rotor pole arc is considered, at first, a conventional structure of a 24/16 switched reluctance three-phase motor arrangement was selected. Then this design has

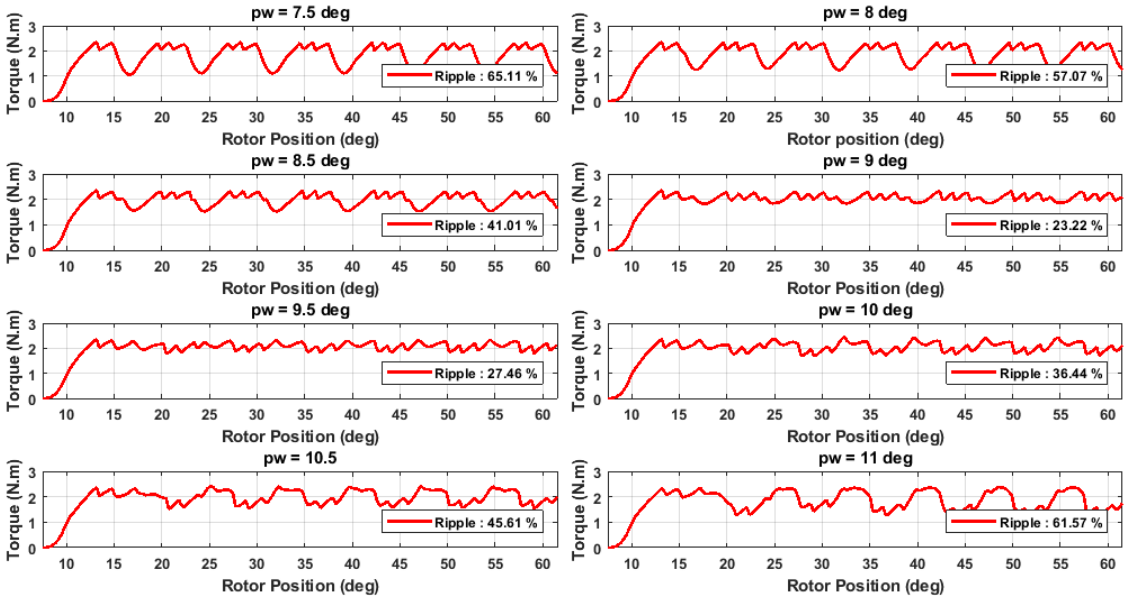

Fig. 8 Torque waveforms for different pulse width.

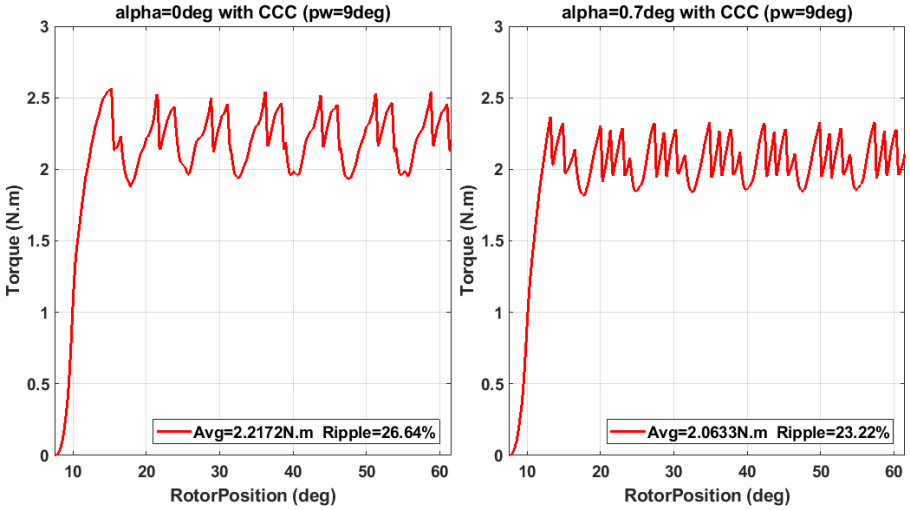

Fig. 9 Torque waveforms of Table 4.

been optimized with the Design of Experimental (DoE) method using finite element software. In order to reduce the single-phase torque ripple, a part of the rotor poles is cut by an arc (α angle) in the direction of rotation. By doing so, the single-phase torque waveform has a lower slope and the single-phase torque ripple is reduced by one percent under dc excitation. In order to reduce the torque ripple significantly, this research has undergone major modifications to its drive control system. To reduce the torque dips in the commutation regions of the phases, the duration of conduction of each phase was increased by increasing the pulse width associated with the phase excitation of the machine. Finally, from the results of the simulation of the pulse width (in degree) which resulted in minimum torque ripple was selected. It is found that by applying this arc (α angle) to the rotor poles and using the selected pulse width for current chopping control, the torque ripple reduced by 3.4% compared to the conventional rotor pole structure. Following optimization, pole shaping and change the pulse width of excitation, it can be said that the total torque ripple of the machine has decreased by 46.7% compared to its conventional design. Also, all simulations are validated with finite element software.

References

[1] J. Hur, G. H. Kang, J. Y. Lee, J. P. Hong, and B. K. Lee, "Design and optimization of high torque, low ripple switched reluctance motor with flux barrier for direct drive," in *39th IAS Annual Meeting. Conference Record of the IEEE Industry Applications Conference*, Vol. 1, 2004.

[2] N. K. Sheth and K. R. Rajagopal, "Optimum pole arcs for a switched reluctance motor for higher torque with reduced ripple," *IEEE Transactions on Magnetics*, Vol. 39, No. 5, pp. 3214–3216, 2003.

[3] Y. Ozoglu, M. Garip, and E. Mese, "New pole tip shapes mitigating torque ripple in short pitched and fully pitched switched reluctance motors," *Electric Power Systems Research*, Vol. 74, No. 1, pp. 95–103, 2005.

[4] G. Li, J. Ojeda, S. Hlioui, E. Hoang, M. Lecrivain, and M. Gabsi, "Modification in rotor pole geometry of mutually coupled switched reluctance machine for torque ripple mitigating," I*EEE Transactions on Magnetics*, Vol. 48, No. 6, pp. 2025–2034, 2012.

[5] J. W. Lee, H. S. Kim, B. I. Kwon, B. T. Kim, "New rotor shape design for minimum torque ripple of SRM using FEM," *IEEE Transactions on Magnetics*, Vol. 40, No. 2, pp. 754–757, 2004.

[6] Y. K. Choi, H. S. Yoon, and C. S. Koh, "Pole-shape optimization of a switched-reluctance motor for torque ripple reduction," *IEEE Transactions on Magnetics*, Vol. 43, No. 4, pp. 1797–1800, 2007.

[7] S. I. Nabeta, I. E. Chabu, L. Lebensztajn, D. A. P. Correa, W. M. Da Silva, and K. Hameyer, "Mitigation of the torque ripple of a switched reluctance motor through a multiobjective optimization," *IEEE Transactions on Magnetics*, Vol. 44, No. 6, pp. 1018–1021, 2008.

[8] D. H. Lee, T. H. Pham, and J. W. Ahn, "Design and operation characteristics of a 4/2 pole high speed SRM for torque ripple reduction," *IEEE Transactions on Industrial Electronics*, Vol. 60, No. 9, pp. 3637–3643, 2013.

[9] F. Daldaban and N. Ustkoyuncu, "Multi-layer switched reluctance motor to reduce torque ripple," *Energy Conversion and Management*, Vol. 49, No. 5, pp. 974–979, 2008.

[10] P. C. Desai, M. Krishnamurthy, N. Schofield, and A. Emadi, "Novel switched reluctance machine configuration with higher number of rotor poles than stator poles: Concept to implementation," *IEEE Transactions on Industrial Electronics*, Vol. 57, No. 2, pp. 649–659, 2010.

[11] C. Sahin, A. E. Amac, M. Karacor, A. Emadi, "Reducing torque ripple of switched reluctance machines by relocation of rotor moulding clinches," *IET Electric Power Applications*, Vol. 6, No. 9, pp. 753–760, 2012.

[12] C. H. Lee, K. T. Chau, C. Liu, T. W. Ching, F. Li, "Mechanical offset for torque ripple reduction for magnetless double-stator doubly salient machine," *IEEE Transactions on Magnetics*, Vol. 50, No. 11, pp. 1–4, 2014.

[13] M. J. Kermanipour and B. Ganji. "Modification in geometric structure of double-sided axial flux switched reluctance motor for mitigating torque ripple," C*anadian Journal of Electrical and Computer Engineering*, Vol. 38, No. 4, pp. 318–322, 2015.

[14] J. W. Jiang, B. Bilgin, and A. Emadi. "Three-phase 24/16 switched reluctance machine for a hybrid electric powertrain," *IEEE Transactions on Transportation Electrification*, Vol. 3, No. 1, pp. 76–85, 2017.

[15] C. Gan, J. Wu, Q. Sun, W. Kong, H. Li, and Y. Hu, "A review on machine topologies and control techniques for low-noise switched reluctance motors in electric vehicle applications," *IEEE Access*, Vol. 6, pp. 31430–31443, 2018.

[16] R. Krishnan, *Switched reluctance motor drives: modeling, simulation, analysis, design, and applications*. CRC Press, 2001.

[17] T. J. E. Miller, *Switched reluctance motors and their control (Monographs in electrical and electronic engineering)*. Clarendon Press, 1993.

[18] T. J. E. Miller, Ed. *Electronic control of switched reluctance machines*. Elsevier, 2001.

[19] E. Elhomdy, G. Li, J. Liu, S. Bukhari, and W. P. Cao, "Design and experimental verification of a 72/48 switched reluctance motor for low-speed direct-drive mining applications," *Energies*, Vol. 11, No. 1 p. 192, 2018.

[20] P. J. Lawrenson, J. M. Stephenson, P. T. Blenkinsop, J. Corda, and N. N. Fulton, "Variable-speed switched reluctance motors," *IET Digital Library*, Vol. 127. No. 4, 1980.

[21] T. J. E. Miller, *Permanent magnet and reluctance motor drives*. Oxford, UK: Oxford Science Publications, 1989.

[22] T. J. E. Miller, "Optimal design of switched reluctance motors," I*EEE Transactions on industrial electronics*, Vol. 49, No. 1, pp. 15–27, 2002.

H. Davari was born in Tehran, Iran, in 1994. He received the B.Sc. degree in power Electrical Engineering from Mazandaran University of Science & Technology (MUST), Babol, Iran in 2016 and he received the M.Sc. degree in power Electronic and Electric Machines Engineering from Semnan University, Semnan, Iran in 2019. His research interests include design and optimization of electric machines and drives.

Y. Alinejad-Beromi was born in Damghan, Iran. He received the B.Sc. degree in Electrical Engineering from K.N.T. University, Tehran, Iran, and the M.Sc. and Ph.D. degrees from UWCC, Cardiff, U.K., in 1989 and 1992, respectively. He is currently an Associate Professor with the Faculty of Electrical and Computer Science Engineering, Semnan University, Semnan, Iran.